

A phase I trial of the MEK inhibitor selumetinib (AZD6244) in pediatric patients with recurrent or refractory low-grade glioma: a Pediatric Brain Tumor Consortium (PBTC) study

Anuradha Banerjee, Regina I. Jakacki, Arzu Onar-Thomas, Shengjie Wu, Theodore Nicolaidis, Tina Young Poussaint, Jason Fangusaro, Joanna Phillips, Arie Perry, David Turner, Michael Prados, Roger J. Packer, Ibrahim Qaddoumi, Sridharan Gururangan, Ian F. Pollack, Stewart Goldman, Lawrence A. Doyle, Clinton F. Stewart, James M. Boyett, Larry E. Kun, and Maryam Fouladi

University of California San Francisco, San Francisco, California (A.B., T.N., J.P., A.P., M.P.); Boston Children's Hospital, Boston, Massachusetts (T.Y.P.); Children's Hospital of Pittsburgh, Pittsburgh, Pennsylvania (R.J., I.F.P.); St Jude Children's Research Hospital, Memphis, Tennessee (A.O.-T., S.W., I.Q., C.F.S., D.T., L.E.K., J.M.B.); Lurie Children's Hospital, Chicago, Illinois (J.F., S.G.); Children's National Medical Center, Washington, DC (R.J.P.); Duke University Medical Center, Durham, North Carolina (S.G.); Cancer Therapy Evaluation Program, National Cancer Institute, Bethesda, Maryland (L.A.D.); Cincinnati Children's Hospital Medical Center, Cincinnati, Ohio (M.F.)

Corresponding Author: Maryam Fouladi, MD, Brain Tumor Center, Cancer and Blood Disorders Institute, Cincinnati Children's Hospital Medical Center, 3333 Burnet Avenue, Cincinnati, OH, 45229 (maryam.fouladi@cchmc.org).

Abstract

Background. Activation of the mitogen-activated protein kinase pathway is important for growth of pediatric low-grade gliomas (LGGs). The aim of this study was to determine the recommended phase II dose (RP2D) and the dose-limiting toxicities (DLTs) of the MEK inhibitor selumetinib in children with progressive LGG.

Methods. Selumetinib was administered orally starting at 33 mg/m²/dose b.i.d., using the modified continual reassessment method. Pharmacokinetic analysis was performed during the first course. BRAF aberrations in tumor tissue were determined by real-time polymerase chain reaction and fluorescence in situ hybridization.

Results. Thirty-eight eligible subjects were enrolled. Dose levels 1 and 2 (33 and 43 mg/m²/dose b.i.d.) were excessively toxic. DLTs included grade 3 elevated amylase/lipase ($n = 1$), headache ($n = 1$), mucositis ($n = 2$), and grades 2–3 rash ($n = 6$). At dose level 0 (25 mg/m²/dose b.i.d., the RP2D), only 3 of 24 subjects experienced DLTs (elevated amylase/lipase, rash, and mucositis). At the RP2D, the median (range) area under the curve ($AUC_{0-\infty}$) and apparent oral clearance of selumetinib were 3855 ng·h/mL (1780 to 7250 ng × h/mL) and 6.5 L × h⁻¹ × m⁻² (3.4 to 14.0 L × h⁻¹ × m⁻²), respectively. Thirteen of 19 tumors had BRAF abnormalities. Among the 5 (20%) of 25 subjects with sustained partial responses, all at the RP2D, 4 had BRAF aberrations, 1 had insufficient tissue. Subjects received a median of 13 cycles (range: 1–26). Fourteen (37%) completed all protocol treatment (26 cycles [$n = 13$], 13 cycles [$n = 1$]) with at least stable disease; 2-year progression-free survival at the RP2D was 69 ± SE 9.8%.

Conclusion. Selumetinib has promising antitumor activity in children with LGG. Rash and mucositis were the most common DLTs.

Key words

low-grade glioma | phase I trial | selumetinib

Low-grade gliomas (LGGs), the most common brain tumors in children, are heterogeneous with a natural history of chronic and/or intermittent progression, particularly if unresectable.¹

Although 5-year overall survival (OS) for patients with LGG is 85%, progression-free survival (PFS) for those with unresectable/residual disease requiring treatment is approximately

Importance of the study

Activation of the mitogen-activated protein kinase pathway, usually via KIAA1549-BRAF fusion or an activating point mutation of BRAF^{V600E}, plays a key role in pediatric LGG pathogenesis. Selumetinib (AZD6244, AstraZeneca) is a potent, selective, orally available, non-ATP-competitive small-molecule inhibitor of MEK-1/2. In this phase I study, we demonstrate that selumetinib is

tolerable and active at the RP2D of 25 mg/m²/dose b.i.d. in children with LGG. Twenty percent of patients had sustained partial responses; patients received a median of 13 courses (range 1–26); 34% completed 26 cycles of therapy with a 2-year progression-free survival at the RP2D of 69 ± SE 9.8%. These phase I results are the basis of ongoing phase II studies in children with LGGs.

40%.² Current treatment strategies, especially radiotherapy, are associated with neurocognitive and neuroendocrine dysfunction, ototoxicity, vasculopathy, and second neoplasms.^{3–8} Chemotherapeutic strategies are often only transiently effective. Novel therapeutic strategies are needed to improve PFS and mitigate these sequelae.

The most common genetic aberrations in pediatric LGG involve activation of the mitogen-activated protein kinase (MAPK) pathway,^{9,10} usually via activation of BRAF through a tandem duplication resulting in KIAA1549-BRAF fusion¹¹ or an activating point mutation of BRAF^{V600E}.¹² Seventy percent to 90% of pilocytic astrocytomas (PA) harbor a BRAF-KIAA1549 fusion¹⁰ and 10%–20% of World Health Organization grades II–IV astrocytomas^{12,13} and 60% of xanthoastrocytomas¹² harbor a BRAF^{V600} mutation. Genetic syndromes such as neurofibromatosis type 1 (NF-1) that activate the Ras/Raf/MAPK pathway are also associated with the development of childhood LGG.^{9,10}

Selumetinib (AZD6244, AstraZeneca) is a potent, selective, orally available, non-ATP-competitive small-molecule inhibitor of MEK-1/2.¹⁴ BRAF^{V600E} PA xenograft model studies demonstrated tumor regression and prolonged event-free survival,¹⁵ while adult studies have demonstrated promising activity in patients with BRAF abnormalities.^{16–22}

We report the results of a phase I trial of selumetinib in children with progressive LGG. The objectives were to estimate the recommended phase II dose (RP2D), describe dose-limiting toxicities (DLTs) and selumetinib pharmacokinetics (PK), assess tumor BRAF aberrations, and describe treatment-related changes in tumor MRI characteristics.

Patients and Methods

Eligibility

Subjects ≥3 and ≤21 years old with progressive or recurrent LGG and Lansky or Karnofsky scores of ≥60 were eligible. Histological verification was required except for those with visual pathway tumors. Subjects must have received ≥1 prior treatment regimen, had to be ≥4 weeks since cytotoxic chemotherapy (6 if nitrosourea), ≥7 days since growth factor (14 if long-acting) or biologic agents, ≥3 half-lives since prior monoclonal antibody, and ≥12 weeks since irradiation. Subjects had to have adequate bone marrow (absolute neutrophil count ≥1000/μL, platelet count ≥100000/μL, hemoglobin ≥8.0 g/dL), renal (age-adjusted normal serum creatinine or glomerular filtration rate ≥70 mL/min/1.73 m²), and liver function (total bilirubin

≤1.5× and alanine aminotransferase ≤2.5× the institutional upper limit of normal for age and albumin ≥3 g/dL). Subjects were excluded if pregnant or lactating or had QTc >450 ms, blood pressure >95th percentile for age, or prior MEK or BRAF inhibitor therapy. Subjects of child-bearing/fathering potential had to consent to birth control, including abstinence. Informed consent and assent were obtained according to institutional guidelines. Institutional review boards of participating institutions maintained protocol approval throughout the study.

Treatment Regimen, Drug Administration, and Dose Escalation

Selumetinib, supplied by AstraZeneca and distributed by the National Cancer Institute (NCI) as 10- and 25-mg capsules, was administered orally twice daily, in 28-day cycles. The protocol initially enrolled subjects ≥12 years of age at a starting dose of 33 mg/m²/dose b.i.d., with planned dose escalations to 95 mg/m²/dose b.i.d. and dose de-escalation to level 0 (25 mg/m²/dose b.i.d.) for toxicity. The protocol was amended to include levels –1 (20 mg/m²/dose b.i.d.) and –2 (15 mg/m²/dose b.i.d.) to allow further dose de-escalation for toxicity and to enroll children 3 to 12 years at the RP2D. Dose escalation was determined by the likelihood-based modified Continual Reassessment Method (CRM) using a 2-parameter logistic model based on dosages adjusted for body surface area with initial cohort sizes of 3 patients at each new dose level. If the cohort was expanded at a given dose beyond 3 patients and the accrual was slow, the algorithm allowed de-escalation based on fewer than 6 patients if warranted by observed number of DLTs. The maximum tolerated dose (MTD) was considered estimated when at least 6 patients were treated at the candidate dose and treating 2 additional patients would not lead to escalation. The details of the algorithm are described by Onar et al,²³ and the rationale of choosing the CRM over other dose finding algorithms and its operating characteristics have been previously described.^{23–26} Patients could receive up to 26 cycles of therapy (~2 y) in the absence of disease progression or adverse events requiring discontinuation of therapy.

Definition of MTD and DLT

The target toxicity level for the MTD was defined as 25% based on DLTs observed during course 1. Toxicities were graded according to the NCI Common Terminology Criteria

for Adverse Events version 4.0. Hematologic DLT was defined as any grade 4 toxicity (except lymphopenia), grade 3 neutropenia with fever, or grade 3 thrombocytopenia with bleeding. Nonhematologic DLT was defined as any grade 3 or 4 toxicity possibly related to selumetinib or any grade 2 toxicity persisting ≥ 7 days that was medically significant or intolerable enough to interrupt/reduce dose.

Definition of Response

Disease evaluations were obtained at baseline; after courses 2, 4, and 6; and after every third course thereafter. Initially, response definitions were: complete response (CR): complete disappearance of *enhancing* tumor and mass effect on MRI with stable or decreasing corticosteroid dose and stable neurologic examination; partial response (PR): $\geq 50\%$ reduction in bidimensional tumor measurements (for CR or PR, response had to be sustained for at least 8 wk); progressive disease (PD): worsening neurologic status or $>25\%$ increase in bidimensional measurements, new lesions, or increasing corticosteroid doses; stable disease (SD): response not meeting criteria for other categories, with stable neurologic examination and corticosteroid dose. Historic definitions of response in pediatric LGG and current standard practice do not rely solely on changes of enhancement patterns, which may not be associated with tumor-volume changes. Indeed, enhancement may completely disappear when significant non-enhancing tumor remains. To conform to more widely accepted response definitions, an amendment clarified MR response definitions—CR: complete tumor disappearance on T2/fluid attenuated inversion recovery (FLAIR) with resolution of any enhancement, no new lesions; and PR: $\geq 50\%$ reduction in bidimensional tumor measurements on T2/FLAIR. SD and PD definitions remained unchanged, with a clarification that increase in T1 postcontrast enhancement alone (without accompanying increase in disease bulk on T2/FLAIR) was not considered tumor progression.

Neuroimaging Correlative Studies

Baseline and on-treatment tumor volume measurements were obtained from the post-gadolinium T1 images and axial FLAIR sequences with user-assisted semi-automated software from the Vitrea workstation (Vital Images). Objective responses were independently verified by the study neuroradiologist (T.Y.P.). Measurements were analyzed in aggregate to interrogate relative changes in tumor size on treatment. Diffusion analyses and region of interest analyses were performed using ImageJ (National Institutes of Health). The mean tumor apparent diffusion coefficient (ADC) value was divided by the mean ADC of a region of interest from normal frontal white matter from the same study.

Pharmacokinetics

Blood samples were collected prior to the first selumetinib dose and up to 24 hours thereafter; the second dose was

held to allow PK assessment of a single selumetinib dose. Selumetinib and N-desmethyl selumetinib concentrations were measured by a validated liquid chromatographic-mass spectrometric assay. Lower limit of quantitation for parent drug and metabolite was 2.0 ng/mL.

The peak plasma concentration (C_{max}) and time to C_{max} (t_{max}) were determined from the plasma concentration-time profile. The log-linear terminal slope (β) was defined by the last 2 measurable concentration-time data points in the serial sampling window. The terminal half-life ($t_{1/2}$) was calculated as $t_{1/2} = \ln(2)/\beta$. The area under the plasma concentration versus time curve from time zero to infinity ($AUC_{0-\infty}$) was calculated using the linear trapezoidal rule. The apparent oral clearance (CL/F) was calculated as the dose normalized by body surface area divided by $AUC_{0-\infty}$. Selumetinib and N-desmethyl selumetinib dose proportionality were assessed by one-way ANOVA on CL/F stratified by dosage.

Tissue Studies for BRAF Aberrations/MAPK Pathway Activation

Phosphorylated extracellular signal-regulated kinase (ERK) was assessed by immunohistochemistry (IHC) (anti-pERK1/2; #4370, Cell Signaling Technology); 1:500 dilution 120 minutes at 37°C using an automated IHC tissue staining process (Benchmark XT, Ventana Medical Systems). Phosphorylated ERK1/2 positivity in tumor cells was scored (J.P.) using a 4-tier system: 0: $<5\%$ tumor cells; 1: $\geq 5\%$ but $<25\%$; 2: $\geq 25\%$ but $<75\%$; 3: $\geq 75\%$. The score denoted the most positive region within at least one high power field at a magnification of 200 \times .

BRAF Fusion Proteins

Unstained slides cut from formalin-fixed paraffin embedded tumor tissue were analyzed for the KIAA1549-BRAF fusion protein by fluorescence in situ hybridization, as previously described.²⁷ The *BRAF-KIAA1549* gene fusion was scored as positive if $>25\%$ showed fusion of one red signal and one green signal resulting in a yellow signal.

BRAF^{V600E} Mutation Detection

The BRAF mutation testing assay utilizes PCR amplification and dye termination sequencing of exon 15 of the BRAF gene using specific PCR primers.

A histologic section of formalin-fixed paraffin embedded tissue is examined by a pathologist to identify an area of tissue with sufficient tumor for detection ($\geq 40\%$ tumor if possible). DNA is extracted from tumor areas on adjacent unstained slides and exon 15 of the BRAF gene is amplified in a PCR reaction. PCR products were purified using the Exo/SAP method. Sequencing reactions were performed using Big Dye v3.1 (Applied Biosystems) with M13 forward and reverse primers. The sequencing products are separated by capillary electrophoresis on an Applied Biosystems 3500XL Genetic Analyzer. Sequence traces were analyzed using Mutation Surveyor (Softgenetics).

Mutations are reported based on National Center for Biotechnology Information Reference Sequence: NM_004333.4.

The limit of detection for Sanger sequencing has been reported to be approximately 20% mutant allele.

Results

Subject Characteristics

Among 38 eligible subjects, 1 progressed during the first course and was inevaluable for estimation of the MTD. **Table 1** summarizes the subject characteristics. The most common histology was PA ($n = 22$). Five had NF-1-associated LGGs. The median number of selumetinib courses was 13 (range: 1–26).

Toxicities

Table 2 summarizes DLTs. Three dose levels were assessed in the ≥ 12 -years-old cohort. At dose level 1 (33 mg/m²/dose

b.i.d.), 1 of 3 subjects experienced a DLT (grade 3 headache), which led to a dose expansion at this dose level. The first subject in the expanded cohort experienced a DLT (grade 2 intolerable rash) and based on 2/4 DLTs, the CRM prompted de-escalation to dose level 0, 25 mg/m²/dose, with no DLTs in 3 subjects, leading to a dose re-escalation to dose level 1. None of the 4 additional subjects enrolled at dose level 1 had a DLT. Since only 2 of 8 subjects at dose level 1 experienced DLTs, escalation to dose level 2 (43 mg/m²/dose b.i.d.) occurred. Two of 3 subjects at dose level 2 experienced DLTs (grade 3 mucositis [$n = 1$]), grade 3 rash [$n = 2$]), rendering this dose too toxic. Thus, the MTD was considered to be 33 mg/m²/dose (dose level 1) and the cohort was expanded; however, 2 of 3 subjects enrolled post-expansion experienced DLTs. Since 4 of 11 patients at dose level 1 had experienced DLTs, this dose level was deemed too toxic. None of 3 subjects experienced a DLT at the de-escalated dose of 25 mg/m²/dose b.i.d., making it the RP2D. As planned, accrual at this dose was expanded to 12 patients by adding 6 additional slots for patients ≥ 12 years old and 12 slots for those aged < 12 years. In the expansion cohort, 3/12 enrolled in the older cohort experienced DLTs. None of the 12 younger subjects enrolled at 25 mg/m²/dose b.i.d. experienced DLTs, rendering 25 mg/m²/dose b.i.d. the RP2D for both cohorts.

Table 3 summarizes all grades 3 and 4 toxicities at least possibly attributable to selumetinib, which most commonly were rash, diarrhea, and creatine phosphokinase (CPK) elevation. One subject, who had an optic pathway glioma and had originally been reported to have grade 4 visual dysfunction, developed worsening grade 4 decreased visual function, without any retinal changes during course 10 of therapy. Seventeen subjects discontinued treatment because of toxicities or patient/physician preference. Two of 3 subjects treated at dose level 2 discontinued treatment after 3 courses following dose reductions. Six of 10 subjects initially assigned to dose level 1 discontinued treatment due to toxicities after 1 to 14 courses, after one or more dose reductions. Among 25 subjects initially assigned to dose level 0, 9 discontinued treatment due to toxicity or patient/physician preference after 1–23 courses, generally after dose reductions. Only 2 of the 9 experienced DLTs in the first course (grade 3 lipase [$n = 1$] that did not resolve despite a dose reduction, and grade 3 mucositis [$n = 1$] in a patient whose therapy was discontinued without an attempt to dose de-escalate). Five of the 7 subjects taken off therapy in later courses either did not experience dose-modifying toxicities and were taken off therapy based on parental/patient ($n = 2$) or physician preference ($n = 1$) or for toxicities that may have been averted or not considered dose modifying based on later amendments. Of the 2 subjects taken off therapy for toxicity during later courses, one experienced asymptomatic grade 3 CPK elevation predating an amendment that excluded grade 3 CPK elevation as a dose-limiting/modifying toxicity and another experienced grade 3 rash/paronychia which may have been averted had a later amendment introducing comprehensive supportive care and treatment guidelines for rash and paronychia been in place.

The treatment duration at each dose level, inpatient dose de-escalations and timing, and reasons for treatment discontinuation are graphically represented in **Figure 1A**.

Table 1 Patient characteristics

Age, y, at study enrollment, median (min, max)	13.3 (5.6, 20.8)	
Prior treatment: median (min, max)		
Chemotherapy/immunotherapy only ($n = 20$)	4 (1–11)	
Chemotherapy/immunotherapy + radiation therapy ($n = 18$)	2.5 (1–8)	
Number of courses of selumetinib: median (min, max)	13 (1–26)	
	Number	Percentage
Gender		
Males	19	50.0
Females	19	50.0
Ethnicity		
Non-Hispanic	34	89.5
Hispanic or Latino	3	7.9
Unknown	1	2.6
Race		
White, non-Hispanic	34	89.5
Black	3	7.9
Unknown	1	2.6
Diagnosis		
Pilocytic astrocytoma	22	57.9
Glioma, not otherwise specified	8	21.1
Astrocytoma, not otherwise specified	4	10.5
Ganglioglioma not otherwise specified	2	5.3
Oligodendroglioma	1	2.6
Pleomorphic xanthoastrocytoma	1	2.6

Table 2 Treatment and DLT summary

Stratum I				
Dose Level (mg/m ² /dose b.i.d.)	Number of Eligible Patients	Number of Evaluable Patients	Number of Patients with DLTs	Description of DLTs
25	25	24	3	Grade 3 amylase/lipase (<i>n</i> = 1) Grade 3 rash (<i>n</i> = 1) Grade 3 mucositis (<i>n</i> = 1)
33	10*	10	4	Grade 3 headache (<i>n</i> = 1) Grade 2 rash (<i>n</i> = 1) Grade 3 rash (<i>n</i> = 2)
43	3	3	2	Grade 3 rash (<i>n</i> = 2) Grade 3 mucositis (<i>n</i> = 1)

* One additional patient was treated at this dose level who was later declared ineligible as a result of a site audit that indicated that patient did not meet protocol criteria for prior/concurrent therapy.

Responses

Five centrally confirmed sustained PRs were reported, all in subjects treated at 25 mg/m²/dose b.i.d. None had NF-1. Among the 5 responders, 2 had *BRAF-KIAA1549* fusion, 1 had a *BRAF*^{V600E} mutation, 1 had both, and 1

Table 3 Grade 3 or 4 toxicities at least possibly attributable to selumetinib, *N* = 38, number of courses = 527

Adverse Events	Grade	
	3	4
Rash maculopapular	8 (7)	
Elevated CPK	7 (3)	1 (1)
Diarrhea	3 (3)	
Rash acneiform	3 (2)	
Decrease in lymphocyte count	2 (2)	
Headache	2 (2)	
Mucositis	2 (2)	
Paronychia	2 (2)	
Elevated lipase	2 (1)	
Elevated alanine aminotransferase increase	1 (1)	
Dry skin	1 (1)	
Infections and infestations	1 (1)	
Hypophosphatemia	1 (1)	
Elevated serum amylase	1 (1)	
Weight gain	1 (1)	
Generalized muscle weakness	1 (1)	
Papulopustular rash	1 (1)	
Fever	1 (1)	
Eye disorders		1 (1)
Dehydration	1 (1)	
Bronchopulmonary hemorrhage		1 (1)

The first number in each cell represents number of episodes for each toxicity and the numbers in parentheses represent number of subjects in whom the toxicity was reported.

had insufficient tissue for evaluation; 4 completed all 26 courses and 1 discontinued therapy due to toxicity after 13 cycles. **Figure 1B** summarizes the response and PFS for all patients. Detailed information on biologic marker status and best response are summarized in supplementary Table A1. Overall, 13 (34%) completed all 26 courses (2 y); 7 additional subjects completed at least 13 cycles (1 y). Among 5 patients with NF-1, 3 completed 26 cycles, one 20 cycles, and one 4 cycles. Among 5 subjects with tissue who had no *BRAF* alterations detected (Table A1), 1 experienced PD after 1 cycle; 3 were taken off therapy due to toxicities after 3, 11, and 24 courses; and 1 completed 26 courses (**Figure 1B**).

Seventeen subjects progressed, 7 on therapy and 10 after discontinuing therapy. Of 17 with PD, 5 experienced clinical progression only; 12 had radiographic progression. Among 10 subjects who progressed while off treatment (including 2 with PRs), progression occurred within 2 (*n* = 2), 3 (*n* = 3), and 7 months (*n* = 4) after discontinuing treatment. Another subject who came off therapy due to toxicity after 2 courses died of PD 1.3 years later. Median follow-up after treatment discontinuation for the 20 subjects who have not progressed is 7.7 months (range: 0–23.8 mo).

Waterfall plots demonstrating reductions in tumor volume from baseline based on minimum tumor size by FLAIR/T2 and by contrast enhancement as measured by central review are in **Figure 2A** and **B**, respectively. A large majority of subjects experienced at least some tumor volume reduction on FLAIR but showed more dramatic and earlier decrease in tumor enhancement.

Volumetric changes in tumor size were quantified by calculating median fold changes between baseline and various treatment time points for subjects. Mixed effects models utilizing longitudinal volume FLAIR and volume contrast enhancement values detected statistically significant decreases over time (volume FLAIR: slope = -0.6592 , $P = .0049$; volume enhancing: slope = -0.6533 , $P = .0003$).

There were significant associations between shorter PFS and increase in tumor volume both on FLAIR ($P = .0031$, hazard ratio [HR] = 1.015) and by enhancement ($P = .0040$, HR = 1.040) as assessed by Cox regression models treating tumor volume as a continuous variable.

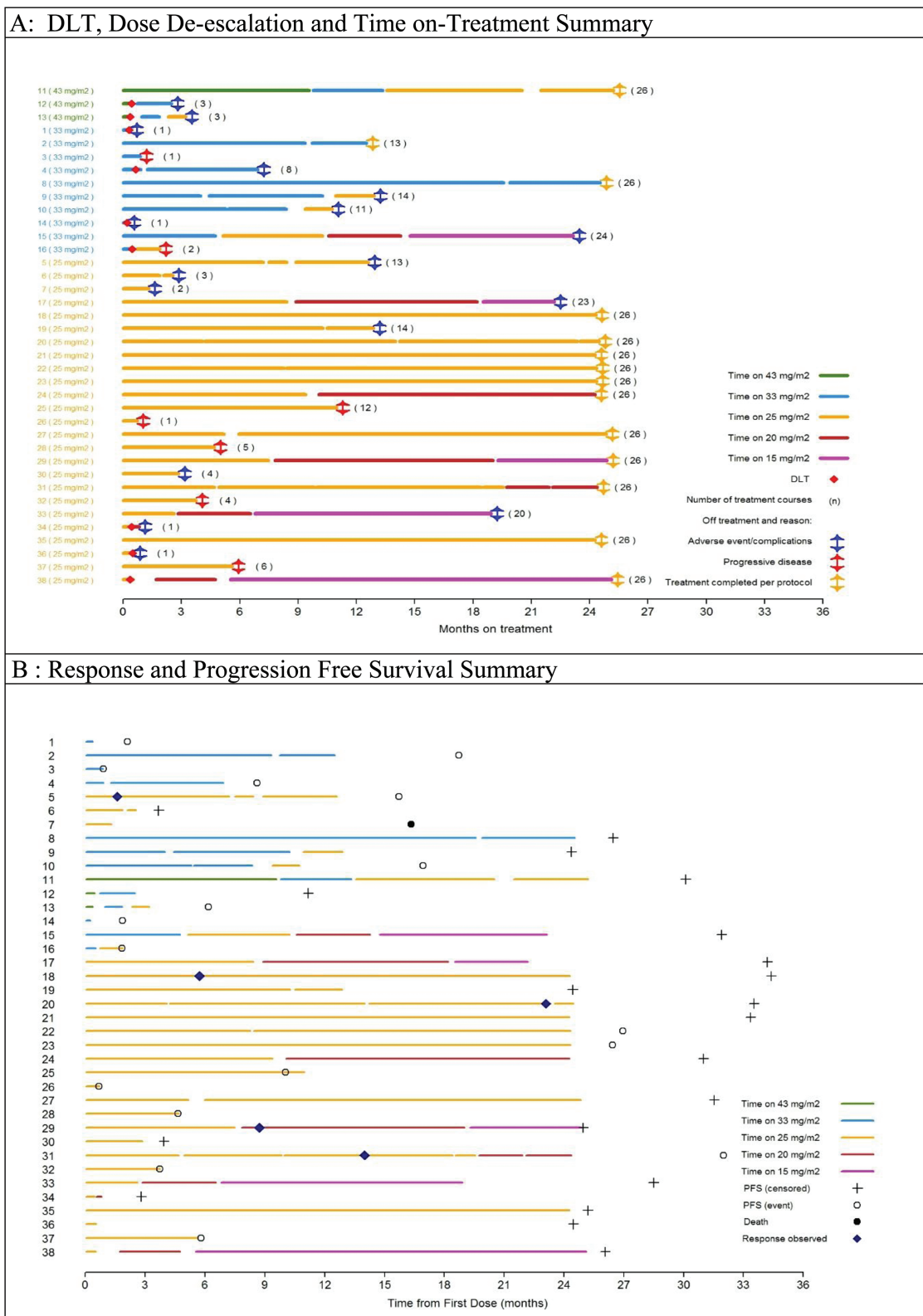


Fig. 1 (A) DLT, dose de-escalation and time on-treatment summary. (B) Response and progression-free survival summary.

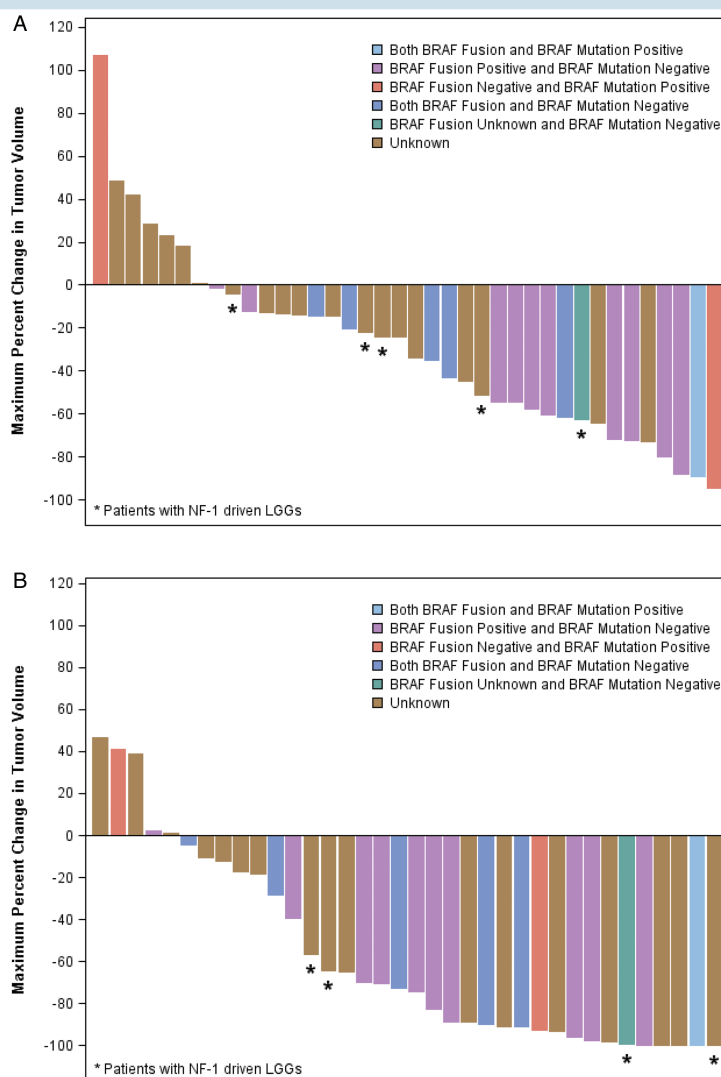


Fig. 2 (A) Percent change in FLAIR volume from baseline by central review. (B) Percent change in contrast-enhancing tumor volume from baseline by central review.

No significant change in diffusion values was detected over time and no association was found between diffusion values and PFS.

An example of the difference in change in FLAIR versus enhancement is shown in supplementary Figure A1. Two-year PFS for the 25 subjects treated at RP2D was $69 \pm SE 9.8\%$ (supplementary Figure A2).

Pharmacokinetics

Selumetinib PK was analyzed for 32 consenting subjects (Table 4). The selumetinib and N-desmethyl selumetinib CL/F values were consistent through all dosage groups (ANOVA; $P = .05$ and $.65$ for parent and metabolite, respectively). The $AUC_{0-\infty}$ of selumetinib and N-desmethyl selumetinib

increased dose-proportionally from dosage level 0 to 2. No significant age dependency in CL/F for selumetinib or N-desmethyl selumetinib was observed (selumetinib $r^2 = .10$, $P = .07$; N-desmethyl selumetinib $r^2 = .02$, $P = .36$).

BRAF Aberrations

Nineteen subjects had tissue for BRAF studies: 10 had *KIAA1549-BRAF* fusion only, 2 had BRAF^{V600E} mutation only, 1 had both, 5 had neither, and 1 had no BRAF^{V600E} mutation but had insufficient tissue to assess *KIAA1549-BRAF* fusion (supplementary Table A1). MAPK pathway signaling was active ($\geq 25\%$ of cells stained positive for ERK1/2 phosphorylation within the most positive region in at least one high power field) in all 20 cases examined.

Table 4 Noncompartmental pharmacokinetic parameters for selumetinib and N-desmethyl selumetinib

	Selumetinib Pharmacokinetic Parameters			N-desmethyl Pharmacokinetic Parameters		
	Selumetinib Dosage (mg/m ²)			AZD6244 Dosage (mg/m ²)		
	25	33	43	25	33	43
<i>n</i> =	23	7	2	23	7	2
<i>C</i> _{max} (ng/mL)	1400 (306–3570)	1750 (372–1860)	3430 (3400–3460)	82 (23–264)	68 (10–92)	152 (107–196)
<i>t</i> _{max} (h)	1.4 (1.0–4.0)	1.5 (1.0–4.0)	1.5 (1.5–1.6)	1.5 (1.0–4.0)	1.5 (1.1–4.0)	1.5 (1.5–1.6)
<i>t</i> _{1/2} (h)	6.5 (4.7–15.8)	10.4 (5.4–23.1)	4.8 (4.3–5.3)	3.2 (1.5–10.1)	10.4 (1.9–29.5)	5.4 (4.8–5.9)
AUC _{0–∞} (ng/mL × h)	3855 (1780–7250)	7325 (4747–14021)	9109 (7978–10231)	112 (276–750)	286 (173–913)	600 (509–691)
CL/F (L/h/m ²)	6.5 (3.4–14.0)	4.5 (2.4–7.0)	4.8 (4.2–5.4)	*91 (33–223)	*115 (36–191)	*77 (73–81)

Values: median (range); *n*: number of patients per dose group; *C*_{max}: observed maximum plasma concentration; *t*_{1/2}: terminal half-life; AUC_{0–∞}: area under the plasma concentration-time curve from time zero to infinity; *CL/F: apparent oral clearance (for N-desmethyl metabolite data, *F* represents a composite of oral bioavailability and fraction metabolized).

Discussion

Selumetinib demonstrated promising activity in children with recurrent LGG, with 20% experiencing sustained PRs at the RP2D of 25 mg/m²/dose b.i.d. Of 5 responders, 4 with available tissue had BRAF aberrations. Compellingly, the 2-year PFS for 25 subjects treated at the RP2D was 69 ± SE 9.8%; 53% of all subjects completed at least one year (13 cycles) of therapy and 34% completed 2 years (26 cycles). Similar to adults, DLTs included rash and mucositis, amylase/lipase elevation, and headache. Chronic selumetinib dosing was poorly tolerated at higher doses. Nine of 24 subjects initially enrolled at the RP2D discontinued treatment because of toxicities in later courses.

Several other agents have shown activity in children with LGGs. Gururangan et al²⁸ reported a 3/30 (10%) PR and 2-year PFS of 49% (30%–67%) for temozolomide compared with 1/21 (5%) PR with 41% SD after 12 cycles in Nicholson et al's study.²⁹ A recent PBTC study reported 2/35 (6%) PR and 2-year PFS of 47.8 ± SE 9.3% for bevacizumab with irinotecan.²⁶ Finally, Bouffet et al³⁰ reported 1 CR and 10 PR (based primarily on *contrast-enhanced imaging* results) in 50 patients (22%), receiving vinblastine with 2-year and 5-year PFS of approximately 62% and 42.3 ± 7.2%, respectively.

In this study, initial response definitions based on reduction of *enhancing* tumor demonstrated 11 PRs among 25 patients at the RP2D (44%). Enhancement in these tumors likely reflects enhanced angiogenesis, vascular endothelial growth factor (VEGF) expression, and VEGF receptor 2 activation (in tumor endothelial cells) characteristic of PA.^{31–33} The modified response criteria, based primarily on tumor volume reduction on T2/FLAIR, reduced the number of centrally reviewed responses to 5 (20%). As the waterfall plots demonstrate, the large majority of subjects experienced a T2/FLAIR tumor-volume reduction with a more dramatic reduction in enhancement (Figure 2). A possible

explanation for the reduction in enhancement is inhibition of MAPK pathway signaling, which is associated with tumor angiogenesis.³⁴ Indeed, MEK inhibitors have been shown to downregulate VEGF production in preclinical models.^{35,36} Similar rapid reductions in enhancement in LGG were observed in the PBTC bevacizumab trial.³⁷ Indeed, given the anti-angiogenic mechanism of action attributed to weekly vinblastine, enhancement-based response definitions in Bouffet et al's study³⁰ may, like our initial results, have overestimated response rates. Three-dimensional ADC histogram analyses of the entire tumor volume may be considered in assessing LGG in future studies.³⁸

This is the first study to describe selumetinib and N-desmethyl selumetinib PK in children. Exposure at dose level 0 is lower than the average (range) AUC at the adult MTD of 75 mg of 6335 ng × h/mL (5260–8510 ng × h/mL) but similar to the adult AUC of 3075 ng × h/mL (1500–6430 ng × h/mL) at a comparable adult dose of 50 mg (or ~29 mg/m²).³⁹ Similar plasma exposures of selumetinib have been demonstrated to inhibit ERK phosphorylation in peripheral blood cells. Plasma N-desmethyl selumetinib concentrations followed a similar PK profile as selumetinib, although exposure was much lower, with *C*_{max} and AUC_{0–∞} values about 6% of parent within each patient.

Of the 5 subjects with PRs, all 4 with available tissue harbored a BRAF aberration. Interestingly, among 4 subjects with early PD (<6 mo), 2 had the *KIAA1549-BRAF* fusion. None of the 5 subjects with NF-1 had a sustained PR, though 3 completed all 26 courses and 4 patients had a reduction in tumor size. In this study, we screened for only the 2 most common genetic alterations in pediatric LGG, *KIAA1549-BRAF* fusions and BRAF^{V600E} mutations. Large-scale sequencing efforts have described other activating mutations in the receptor tyrosine kinase/Ras/Raf/MAPK pathway in LGGs in genes including *FGFR1*, *NTRK2*, *BRAF*, *RAF1*, *PTPN11*, *NF-1*, and *RAS*.⁴⁰ While we did not screen for these additional mutations, our IHC results indicate MAPK pathway activation in all tumors tested.

The level and type of pathway aberration is critical in determining therapy with targeted agents. Rapid disease progression, reported in children with LGG with BRAF fusions treated with the BRAF inhibitor sorafenib⁴¹ may be explained by the fact that the fusion kinase in cells expressing KIAA1549-BRAF functions as a homodimer, rendering them resistant to BRAF inhibition and displaying paradoxical activation of MAPK signaling.⁴²

In summary, selumetinib is tolerable and active at the RP2D of 25 mg/m²/dose b.i.d. in children with LGG. The ongoing PBTC phase II trial stratifies subjects based on histology, BRAF aberration, and NF-1, to allow correlation with tumor response and PFS. Planned targeted-genomic analysis in this study will allow larger-scale assessment of mechanisms of sensitivity and resistance in this patient population.

Supplementary Material

Supplementary material is available at *Neuro-Oncology* online.

Funding

This work was supported in part by grant U01 CA 81457 from the National Institutes of Health to the Pediatric Brain Tumor Consortium and the American-Lebanese Syrian Associated Charities (ALSAC).

Acknowledgments

We acknowledge the clinical research assistant support of Wint Swe and Stacy Richardson.

References

- Dolecek TA, Propp JM, Stroup NE, et al. CBTRUS statistical report: primary brain and central nervous system tumors diagnosed in the United States in 2005–2009. *Neuro Oncol*. 2012;14 Suppl 5:v1–v49.
- Ater JL, Zhou T, Holmes E, et al. Randomized study of two chemotherapy regimens for treatment of low-grade glioma in young children: a report from the Children's Oncology Group. *J Clin Oncol*. 2012;30(21):2641–2647.
- Ris MD, Beebe DW, Armstrong FD, et al.; Children's Oncology Group. Cognitive and adaptive outcome in extracerebellar low-grade brain tumors in children: a report from the Children's Oncology Group. *J Clin Oncol*. 2008;26(29):4765–4770.
- Tacke U, Karger D, Spreer J, et al. Incidence of vasculopathy in children with hypothalamic/chiasmatic gliomas treated with brachytherapy. *Childs Nerv Syst*. 2011;27(6):961–966.
- Perkins SM, Fei W, Mitra N, et al. Late causes of death in children treated for CNS malignancies. *J Neurooncol*. 2013;115(1):79–85.
- Greenberger BA, Pulsifer MB, Ebb DH, et al. Clinical outcomes and late endocrine, neurocognitive, and visual profiles of proton radiation for pediatric low-grade gliomas. *Int J Radiat Oncol Biol Phys*. 2014;89(5):1060–1068.
- Bandopadhyay P, Bergthold G, London WB, et al. Long-term outcome of 4040 children diagnosed with pediatric low-grade gliomas: an analysis of the surveillance epidemiology and end results (SEER) database. *Pediatr Blood Cancer*. 2014;61(7):1173–1179.
- Grill J, Couanet D, Cappelli C, et al. Radiation-induced cerebral vasculopathy in children with neurofibromatosis and optic pathway glioma. *Ann Neurol*. 1999;45(3):393–396.
- Chen YH, Gutmann DH. The molecular and cell biology of pediatric low-grade gliomas. *Oncogene*. 2014;33(16):2019–2026.
- Zhang J, Wu G, Miller CP, et al.; St. Jude Children's Research Hospital–Washington University Pediatric Cancer Genome Project. Whole-genome sequencing identifies genetic alterations in pediatric low-grade gliomas. *Nat Genet*. 2013;45(6):602–612.
- Jones DT, Kocalkowski S, Liu L, et al. Tandem duplication producing a novel oncogenic BRAF fusion gene defines the majority of pilocytic astrocytomas. *Cancer Res*. 2008;68(21):8673–8677.
- Schindler G, Capper D, Meyer J, et al. Analysis of BRAF V600E mutation in 1320 nervous system tumors reveals high mutation frequencies in pleomorphic xanthoastrocytoma, ganglioglioma and extra-cerebellar pilocytic astrocytoma. *Acta Neuropathol*. 2011;121(3):397–405.
- Forshew T, Tatevossian RG, Lawson AR, et al. Activation of the ERK/MAPK pathway: a signature genetic defect in posterior fossa pilocytic astrocytomas. *J Pathol*. 2009;218(2):172–181.
- Yeh TC, Marsh V, Bernat BA, et al. Biological characterization of ARRY-142886 (AZD6244), a potent, highly selective mitogen-activated protein kinase kinase ½ inhibitor. *Clin Cancer Res*. 2007;13(5):1576–1583.
- Kolb EA, Gorlick R, Houghton PJ, et al. Initial testing (stage 1) of AZD6244 (ARRY-142886) by the Pediatric Preclinical Testing Program. *Pediatr Blood Cancer*. 2010;55(4):668–677.
- Kirkwood JM, Bastholt L, Robert C, et al. Phase II, open-label, randomized trial of the MEK1/2 inhibitor selumetinib as monotherapy versus temozolomide in patients with advanced melanoma. *Clin Cancer Res*. 2012;18(2):555–567.
- Catalanotti F, Solit DB, Pulitzer MP, et al. Phase II trial of MEK inhibitor selumetinib (AZD6244, ARRY-142886) in patients with BRAFV600E/K-mutated melanoma. *Clin Cancer Res*. 2013;19(8):2257–2264.
- Hochster HS, Uboha N, Messersmith W, et al. Phase II study of selumetinib (AZD6244, ARRY-142886) plus irinotecan as second-line therapy in patients with K-RAS mutated colorectal cancer. *Cancer Chemother Pharmacol*. 2015;75(1):17–23.
- Adjei AA, Cohen RB, Franklin W, et al. Phase I pharmacokinetic and pharmacodynamic study of the oral, small-molecule mitogen-activated protein kinase kinase ½ inhibitor AZD6244 (ARRY-142886) in patients with advanced cancers. *J Clin Oncol*. 2008;26(13):2139–2146.
- Robert C, Dummer R, Gutzmer R, et al. Selumetinib plus dacarbazine versus placebo plus dacarbazine as first-line treatment for BRAF-mutant metastatic melanoma: a phase 2 double-blind randomised study. *Lancet Oncol*. 2013;14(8):733–740.
- Farley J, Brady WE, Vathipadiekal V, et al. Selumetinib in women with recurrent low-grade serous carcinoma of the ovary or peritoneum: an open-label, single-arm, phase 2 study. *Lancet Oncol*. 2013;14(2):134–140.
- Carvajal RD, Sosman JA, Quevedo JF, et al. Effect of selumetinib vs chemotherapy on progression-free survival in uveal melanoma: a randomized clinical trial. *JAMA*. 2014;311(23):2397–2405.
- Onar A, Kocak M, Boyett JM. Continual reassessment method vs. traditional empirically based design: modifications motivated by phase I trials in pediatric oncology by the pediatric brain tumor consortium. *J Biopharm Stat*. 2009;19(3):437–455.

24. Wages NA, Conaway MR, O'Quigley J. Performance of two-stage continual reassessment method relative to an optimal benchmark. *Clin Trials*. 2013;10(6):862–875.
25. O'Quigley J, Conaway M. Continual reassessment and related dose-finding designs. *Stat Sci*. 2010;25(2):202–216.
26. Iasonos A, O'Quigley J. Adaptive dose-finding studies: a review of model-guided phase I clinical trials. *J Clin Oncol*. 2014;32(23):2505–2511.
27. Rodriguez FJ, Schniederjan MJ, Nicolaidis T, et al. High rate of concurrent BRAF-KIAA1549 gene fusion and 1p deletion in disseminated oligodendroglioma-like leptomeningeal neoplasms (DOLN). *Acta Neuropathol*. 2015;129(4):609–610.
28. Gururangan S, Fisher MJ, Allen JC, et al. Temozolomide in children with progressive low-grade glioma. *Neuro Oncol*. 2007;9(2):161–168.
29. Nicholson HS, Kretschmar CS, Krailo M, et al. Phase 2 study of temozolomide in children and adolescents with recurrent central nervous system tumors: a report from the Children's Oncology Group. *Cancer*. 2007;110(7):1542–1550.
30. Bouffet E, Jakacki R, Goldman S, et al. Phase II study of weekly vinblastine in recurrent or refractory pediatric low-grade glioma. *J Clin Oncol*. 2012;30(12):1358–1363.
31. Sie M, de Bont ES, Scherpen FJ, et al. Tumour vasculature and angiogenic profile of paediatric pilocytic astrocytoma; is it much different from glioblastoma? *Neuropathol Appl Neurobiol*. 2010;36(7):636–647.
32. Leung SY, Chan AS, Wong MP, et al. Expression of vascular endothelial growth factor and its receptors in pilocytic astrocytoma. *Am J Surg Pathol*. 1997;21(8):941–950.
33. Sikkema AH, de Bont ES, Molema G, et al. Vascular endothelial growth factor receptor 2 (VEGFR-2) signalling activity in paediatric pilocytic astrocytoma is restricted to tumour endothelial cells. *Neuropathol Appl Neurobiol*. 2011;37(5):538–548.
34. Sodhi A, Montaner S, Miyazaki H, et al. MAPK and Akt act cooperatively but independently on hypoxia inducible factor-1alpha in rasV12 upregulation of VEGF. *Biochem Biophys Res Commun*. 2001;287(1):292–300.
35. Ciuffreda L, Del Bufalo D, Desideri M, et al. Growth-inhibitory and antiangiogenic activity of the MEK inhibitor PD0325901 in malignant melanoma with or without BRAF mutations. *Neoplasia*. 2009;11(8):720–731.
36. Gao JH, Wang CH, Tong H, et al. Targeting inhibition of extracellular signal-regulated kinase kinase pathway with AZD6244 (ARRY-142886) suppresses growth and angiogenesis of gastric cancer. *Sci Rep*. 2015;5:16382.
37. Gururangan S, Fangusaro J, Poussaint TY, et al. Efficacy of bevacizumab plus irinotecan in children with recurrent low-grade gliomas—a Pediatric Brain Tumor Consortium study. *Neuro Oncol*. 2014;16(2):310–317.
38. Poussaint TY, Vajapeyam S, Ricci KI, et al. Apparent diffusion coefficient histogram metrics correlate with survival in diffuse intrinsic pontine glioma: a report from the pediatric brain tumor consortium. *Neuro Oncol*. 2016;18(5):725–734.
39. Banerji U, Camidge DR, Verheul HM, et al. The first-in-human study of the hydrogen sulfate (Hyd-sulfate) capsule of the MEK1/2 inhibitor AZD6244 (ARRY-142886): a phase I open-label multicenter trial in patients with advanced cancer. *Clin Cancer Res*. 2010;16(5):1613–1623.
40. Jones DT, Hutter B, Jäger N, et al.; International Cancer Genome Consortium PedBrain Tumor Project. Recurrent somatic alterations of FGFR1 and NTRK2 in pilocytic astrocytoma. *Nat Genet*. 2013;45(8):927–932.
41. Karajannis MA, Legault G, Fisher MJ, et al. Phase II study of sorafenib in children with recurrent or progressive low-grade astrocytomas. *Neuro Oncol*. 2014;16(10):1408–1416.
42. Sievert AJ, Lang SS, Boucher KL, et al. Paradoxical activation and RAF inhibitor resistance of BRAF protein kinase fusions characterizing pediatric astrocytomas. *Proc Natl Acad Sci U S A*. 2013;110(15):5957–5962.